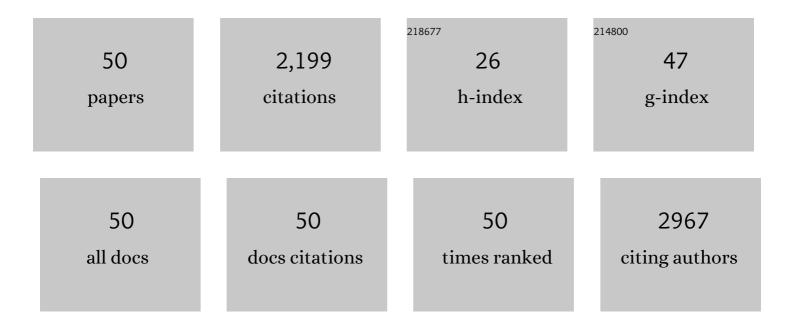
## Zheng Guo

## List of Publications by Year in descending order

Source: https://exaly.com/author-pdf/5185762/publications.pdf Version: 2024-02-01



ZHENC CUO

#	Article	IF	CITATIONS
1	Porous Pb-Doped ZnO Nanobelts with Enriched Oxygen Vacancies: Preparation and Their Chemiresistive Sensing Performance. Chemosensors, 2022, 10, 96.	3.6	9
2	SnO <sub>2</sub> Nanostructures Exposed with Various Crystal Facets for Temperature-Modulated Sensing of Volatile Organic Compounds. ACS Applied Nano Materials, 2022, 5, 10636-10644.	5.0	12
3	Polyoxometalate-assisted in situ growth of ZnMoO4 on ZnO nanofibers for the selective detection of ppb-level acetone. Sensors and Actuators B: Chemical, 2022, 369, 132354.	7.8	8
4	Ag nanoparticles anchored onto porous CuO nanobelts for the ultrasensitive electrochemical detection of dopamine in human serum. Sensors and Actuators B: Chemical, 2021, 327, 128878.	7.8	68
5	Cation-exchange synthesis of PbSe/ZnSe hetero-nanobelts with enhanced near-infrared photoelectronic performance. Nanotechnology, 2021, 32, 335504.	2.6	2
6	Selectively enhanced gas-sensing performance to n-butanol based on uniform CdO-decorated porous ZnO nanobelts. Sensors and Actuators B: Chemical, 2021, 334, 129667.	7.8	18
7	PEGylated AdipoRon derivatives improve glucose and lipid metabolism under insulinopenic and high-fat diet conditions. Journal of Lipid Research, 2021, 62, 100095.	4.2	13
8	A Temperature-Modulated Gas Sensor Based on CdO-Decorated Porous ZnO Nanobelts for the Recognizable Detection of Ethanol, Propanol, and Isopropanol. IEEE Sensors Journal, 2021, 21, 25590-25596.	4.7	12
9	Framework-derived Fe2O3/Mn3O4 nanocubes as electrochemical catalyst for simultaneous analysis of Cu(II) and Hg(II). Electrochimica Acta, 2021, 399, 139412.	5.2	10
10	Porous CuO nanobelts assembly film for nonenzymatic electrochemical determination of glucose with High fabrication repeatability and sensing stability. Sensors and Actuators B: Chemical, 2020, 307, 127639.	7.8	36
11	Regulation of intrinsic physicochemical properties of metal oxide nanomaterials for energy conversion and environmental detection applications. Journal of Materials Chemistry A, 2020, 8, 17326-17359.	10.3	33
12	A direct Z-scheme ZnS/Co <sub>9</sub> S <sub>8</sub> heterojunction-based photoelectrochemical sensor for the highly sensitive and selective detection of chlorpyrifos. Environmental Science: Nano, 2020, 7, 753-763.	4.3	26
13	Cation-exchange strategy for a colorimetric paper sensor: Belt-like ZnSe nanoframes toward visual determination of heavy metal ions. Sensors and Actuators B: Chemical, 2020, 312, 128013.	7.8	17
14	Enhanced chemiresistive sensing performance of well-defined porous CuO-doped ZnO nanobelts toward VOCs. Nanoscale Advances, 2019, 1, 3900-3908.	4.6	14
15	Electrochemical monitoring of persistent toxic substances using metal oxide and its composite nanomaterials: Design, preparation, and application. TrAC - Trends in Analytical Chemistry, 2019, 119, 115636.	11.4	44
16	Porous Singleâ€Crystalline CdSe Nanobelts: Cationâ€Exchange Synthesis and Highly Selective Photoelectric Sensing toward Cu <sup>2+</sup> . Chemistry - A European Journal, 2018, 24, 9877-9883.	3.3	16
17	Surface Fe(II)/Fe(III) Cycle Promoted Ultra-Highly Sensitive Electrochemical Sensing of Arsenic(III) with Dumbbell-Like Au/Fe <sub>3</sub> O <sub>4</sub> Nanoparticles. Analytical Chemistry, 2018, 90, 4569-4577.	6.5	105
18	Noble-Metal-Free Co <sub>0.6</sub> Fe <sub>2.4</sub> O <sub>4</sub> Nanocubes Self-Assembly Monolayer for Highly Sensitive Electrochemical Detection of As(III) Based on Surface Defects. Analytical Chemistry, 2018, 90, 1263-1272.	6.5	66

Zheng Guo

#	Article	IF	CITATIONS
19	Cation-Exchange Synthesis of Cu <sub>2</sub> Se Nanobelts and Thermal Conversion to Porous CuO Nanobelts with Highly Selective Sensing toward H <sub>2</sub> S. ACS Applied Nano Materials, 2018, 1, 245-253.	5.0	25
20	Insights into diverse performance for the electroanalysis of Pb(II) on Fe2O3 nanorods and hollow nanocubes: Toward analysis of adsorption sites. Electrochimica Acta, 2018, 288, 42-51.	5.2	34
21	Size-tunable Ag nanoparticles sensitized porous ZnO nanobelts: controllably partial cation-exchange synthesis and selective sensing toward acetic acid. Nanotechnology, 2018, 29, 445501.	2.6	14
22	In Situ Underwater Laser-Induced Breakdown Spectroscopy Analysis for Trace Cr(VI) in Aqueous Solution Supported by Electrosorption Enrichment and a Gas-Assisted Localized Liquid Discharge Apparatus. Analytical Chemistry, 2017, 89, 5557-5564.	6.5	35
23	Competitive adsorption behavior toward metal ions on nano-Fe/Mg/Ni ternary layered double hydroxide proved by XPS: Evidence of selective and sensitive detection of Pb(II). Journal of Hazardous Materials, 2017, 338, 1-10.	12.4	72
24	A simplified electrochemical instrument equipped with automated flow-injection system and network communication technology for remote online monitoring of heavy metal ions. Journal of Electroanalytical Chemistry, 2017, 791, 49-55.	3.8	21
25	Hierarchical Morphology-Dependent Gas-Sensing Performances of Three-Dimensional SnO <sub>2</sub> Nanostructures. ACS Sensors, 2017, 2, 102-110.	7.8	138
26	Functionalized porous Si nanowires for selective and simultaneous electrochemical detection of Cd(II) and Pb(II) ions. Electrochimica Acta, 2016, 211, 998-1005.	5.2	55
27	Porous and single-crystalline ZnO nanobelts: fabrication with annealing precursor nanobelts, and gas-sensing and optoelectronic performance. Nanotechnology, 2016, 27, 355702.	2.6	32
28	Electrochemical Detection of Trace Arsenic(III) by Nanocomposite of Nanorod-Like α-MnO <sub>2</sub> Decorated with â^1⁄45 nm Au Nanoparticles: Considering the Change of Arsenic Speciation. Analytical Chemistry, 2016, 88, 9720-9728.	6.5	98
29	An atomically thick titanium phosphate thin layer with enhancing electrochemical sensitivity toward Pb( <scp>ii</scp> ). RSC Advances, 2016, 6, 72975-72984.	3.6	11
30	Tunable nanogap devices for ultra-sensitive electrochemical impedance biosensing. Analytica Chimica Acta, 2016, 905, 58-65.	5.4	9
31	Adsorbent Assisted <i>in Situ</i> Electrocatalysis: An Ultra-Sensitive Detection of As(III) in Water at Fe <sub>3</sub> O <sub>4</sub> Nanosphere Densely Decorated with Au Nanoparticles. Analytical Chemistry, 2016, 88, 1154-1161.	6.5	90
32	Organic Pollutants: A Versatile Environmental Impedimetric Sensor for Ultrasensitive Determination of Persistent Organic Pollutants (POPs) and Highly Toxic Inorganic Ions (Adv. Sci. 5/2015). Advanced Science, 2015, 2, .	11.2	0
33	Cation Exchange Synthesis and Unusual Resistive Switching Behaviors of Ag <sub>2</sub> Se Nanobelts. Small, 2015, 11, 6285-6294.	10.0	26
34	Ag-decorated ultra-thin porous single-crystalline ZnO nanosheets prepared by sunlight induced solvent reduction and their highly sensitive detection of ethanol. Sensors and Actuators B: Chemical, 2015, 209, 975-982.	7.8	87
35	Ultrasensitive and Ultraselective Impedimetric Detection of Cr(VI) Using Crown Ethers as High-Affinity Targeting Receptors. Analytical Chemistry, 2015, 87, 1991-1998.	6.5	61
36	New Strategy for Rapid Detection of the Simulants of Persistent Organic Pollutants Using Gas Sensor Based on 3-D Porous Single-Crystalline ZnO Nanosheets. IEEE Sensors Journal, 2015, 15, 3668-3674.	4.7	12

Zheng Guo

#	Article	IF	CITATIONS
37	Electroadsorption-Assisted Direct Determination of Trace Arsenic without Interference Using Transmission X-ray Fluorescence Spectroscopy. Analytical Chemistry, 2015, 87, 8503-8509.	6.5	18
38	Flower-like hierarchical structures consisting of porous single-crystalline ZnO nanosheets and their gas sensing properties to volatile organic compounds (VOCs). Journal of Alloys and Compounds, 2015, 626, 124-130.	5.5	99
39	A molecular-gap device for specific determination of mercury ions. Scientific Reports, 2013, 3, 3115.	3.3	24
40	Hydroxylation/carbonylation carbonaceous microspheres: A route without the need for an external functionalization to a "hunter―of lead(II) for electrochemical detection. Electrochimica Acta, 2013, 87, 46-52.	5.2	17
41	Sensitive and selective electrochemical detection of dopamine using an electrode modified with carboxylated carbonaceous spheres. Analyst, The, 2013, 138, 2683.	3.5	70
42	A pH sensor with a double-gate silicon nanowire field-effect transistor. Applied Physics Letters, 2013, 102, .	3.3	46
43	Transport Phenomena and Conduction Mechanism of Individual Crossâ€Junction SnO <sub>2</sub> Nanobelts. Small, 2013, 9, 2678-2683.	10.0	6
44	Effects of the oxygen vacancy concentration in InGaZnO-based resistance random access memory. Applied Physics Letters, 2012, 101, .	3.3	55
45	Hollow CuO nanospheres uniformly anchored on porous Si nanowires: preparation and their potential use as electrochemical sensors. Nanoscale, 2012, 4, 7525.	5.6	55
46	T-shaped SnO2 nanowire current splitter. Materials Today, 2011, 14, 42-49.	14.2	5
47	Templating Synthesis of SnO <sub>2</sub> Nanotubes Loaded with Ag <sub>2</sub> O Nanoparticles and Their Enhanced Gas Sensing Properties. Advanced Functional Materials, 2011, 21, 2049-2056.	14.9	130
48	Novel porous single-crystalline ZnO nanosheets fabricated by annealing ZnS(en) <sub>0.5</sub> (en =) Tj ETQq0 C Nanotechnology, 2009, 20, 125501.	0 rgBT /0 2.6	Overlock 10 137
49	Template synthesis, organic gas-sensing and optical properties of hollow and porous In <sub>2</sub> O <sub>3</sub> nanospheres. Nanotechnology, 2008, 19, 345704.	2.6	106
50	Highly porous CdO nanowires: preparation based on hydroxy- and carbonate-containing cadmium compound precursor nanowires, gas sensing and optical properties. Nanotechnology, 2008, 19, 245611.	2.6	102